

Optical Properties of Dilute Ag-In Alloys*

R. M. MORGAN† AND D. W. LYNCH

Institute for Atomic Research and Department of Physics, Iowa State University, Ames, Iowa 50010

(Received 21 March 1968)

The optical constants of silver and five dilute silver-indium alloys (<5% In) were determined from reflectance and transmittance measurements in the spectral region between 3.35 and 4.28 eV on vacuum-evaporated films. The data are consistent with the assumption that the onset of interband absorption in silver arises primarily from direct interband transitions from the d band near L_3 to the Fermi surface, but with a small, though not insignificant, contribution due to direct transitions from the conduction band near L_2' to the conduction band near L_1 . The changes in the complex dielectric constant induced by alloying were interpreted to indicate a shift of the $L_3 \rightarrow E_F$ transition to higher energy and a shift of the $L_2' \rightarrow L_1$ transition to lower energy. Because contributions to the dielectric constant of the two transitions overlap and because of the limited energy range investigated, no firm estimates of the magnitudes of the shifts could be made, but it seems clear that the $L_2'-L_1$ energy gap decreases as indium is added to silver. The strength of the interband absorption in the alloys at energies below that of the edge in silver appeared to be too strong to be accounted for by indirect transitions. Alloying-induced changes in the energy-loss function showed that the relatively undamped plasma resonance in silver near 3.8 eV becomes strongly damped as indium is added. The increase in damping was attributed partly to a decrease in the conduction-electron relaxation time, and partly to the shift of interband transitions so that they occur at the plasma energy. Data from measurements on films cooled to liquid-helium temperature showed some sharpening of structure in the complex dielectric constant and of the peak in the loss function.

INTRODUCTION

THE optical constants of a metal characterize the response of the electrons in the metal to an applied electric field at optical frequencies. The response often can be divided into three parts: one due to one-electron excitations of the electrons in the conduction band, one due to the excitation of collective modes of oscillation of the conduction-band electrons, and one due to exciting interband transitions. In some metals the above three effects fall into wavelength regions sufficiently separated that the study of each effect separately is possible. One such metal is silver,^{1,2} the optical constants of which are particularly interesting because of this separability, and because the collective effects occur in a particularly convenient wavelength region.

It is well known that studies of the optical properties of metals and calculations of the band structures of metals complement each other. The optical constants cannot be interpreted in any detail without some knowledge of the band structure, while band-structure calculations can be checked, and parameters adjusted, by comparison with observed optical-transition energies and oscillator strengths. Although there exists no good general theory of alloys, one has the intuitive feeling that studies of dilute alloys can somehow give information about the band structure of the pure solvent, even though alloying may alter the band structure. Moreover, optical studies may be used to sort out conflicting theories of alloys.

Studies of the optical constants of dilute Ag-In alloys

were undertaken to confirm the assignment of the transitions responsible for the first interband absorption edge, to study the effect of alloying on the plasma oscillations, and to provide data with which to test various "theories of alloys." We find that the first interband transition in pure silver can be interpreted as a composite of a strong transition from the upper d band to the Fermi surface (near $L_3 \rightarrow L_2'$) and a weak transition from the Fermi surface to a higher conduction band (near $L_2' \rightarrow L_1$), as suggested by Beaglehole³ and by Mueller and Phillips.⁴ No clear evidence for indirect transitions was found. The effects of alloying on the plasma oscillations in silver are made clear, and plasmon damping in these alloys is seen to arise from both interband and intraband transitions.

OPTICAL PROPERTIES OF SILVER AND COPPER

The complex dielectric constant of a metal can be written as the sum of an intraband (free-carrier) term and an interband term:

$$\tilde{\epsilon}(\omega) = \tilde{\epsilon}^f(\omega) + \tilde{\epsilon}^b(\omega). \quad (1)$$

Classical theory gives

$$\begin{aligned} \tilde{\epsilon}^f(\omega) &= \epsilon_1^f(\omega) + i\epsilon_2^f(\omega) \\ &= 1 - \frac{\omega_p^2 \tau^2}{1 + \omega^2 \tau^2} + i \frac{\omega_p^2 \tau \omega^{-1}}{1 + \omega^2 \tau^2}, \end{aligned} \quad (2)$$

where $\omega_p = (4\pi N e^2 / m^*)^{1/2}$ is the plasma frequency and τ is a relaxation time for conduction-band electrons. N is the concentration of free electrons and m^* is an effective

* Work performed in the Ames Laboratory of the U. S. Atomic Energy Commission. Contribution No. 2282.

† Present address: Christian Brothers College, Memphis, Tenn. 38104.

¹ E. A. Taft and H. R. Philipp, Phys. Rev. **121**, 1100 (1961).

² H. Ehrenreich and H. R. Philipp, Phys. Rev. **128**, 1622 (1962).

³ D. Beaglehole, Proc. Phys. Soc. (London) **85**, 1007 (1965); **87**, 461 (1966).

⁴ F. M. Mueller and J. C. Phillips, Phys. Rev. **157**, 600 (1967).

mass which, for silver, is close to the free-electron mass. τ can be found from the dc conductivity. Equation (2) fits the optical data for silver⁵ for $\hbar\omega \lesssim 1$ eV, using the dc value for τ . Between about 1 and 3.5 eV, τ appears only in ϵ_2^f and it must be smaller than the dc value if Eq. (2) is to fit the data,² assuming negligible ϵ_2^b in this energy region.

If $\omega\tau \gg 1$, Eq. (2) reduces to

$$\tilde{\epsilon}^f(\omega) = 1 - \frac{\omega_p^2}{\omega^2} + \frac{i\omega_p^2}{\omega^3\tau}, \quad (3)$$

and $\tilde{\epsilon} = 0$ at $\omega = \omega_p[1 - i/(2\omega_p\tau)] \approx \omega_p$. At ω_p , $\epsilon_1^f = 0$. For the conduction-band electron concentration in silver, $\hbar\omega_p = 9.2$ eV, but from experiment, $\epsilon_1(\omega)$ goes through zero at about 3.8 eV. The large shift arises⁶ from the interband contribution to $\tilde{\epsilon}$.

$\epsilon_2^b(\omega)$ will rise above zero when ω is high enough to allow an interband transition, while $\epsilon_1^b(\omega)$ departs from its low-frequency constant value at photon energies up to a few eV below that of the first interband transition. In the case of silver, the energy of the first interband transition, 3.9 eV, and its strength are within the range of values needed to shift the zero of ϵ_1 from 9.2 eV to a far lower energy, 3.8 eV. (In copper, interband transitions fail to produce such a dramatic shift. The observed plasma frequency is at 7.5 eV instead of the free-electron-gas value of 9.3 eV.²)

A plasma oscillation or plasmon is a long-wavelength collective longitudinal oscillation of electron density in the conduction band. For a free-electron gas the (complex) frequency at which $\tilde{\epsilon}(\omega) = 0$ is the frequency of a well-defined plasma oscillation provided the imaginary part of this frequency is small compared to the real part.⁷ Such is the case in pure silver, and an implicit equation for the frequency of the plasma oscillations ω_0 is

$$\omega_0 = \omega_p / [1 + \epsilon_1^b(\omega_0)]^{1/2}, \quad (4)$$

where $\omega_0\tau \gg 1$ and $\epsilon_2^b(\omega_0) \approx 0$. The collective motion of the electrons is now the result of their mutual Coulomb repulsion screened by the polarization of the d -band electrons responsible for the interband absorption. Equation (4) is valid for silver but not for the alloys we have studied. For them, $\epsilon_2^b(\omega_0)$ is not negligible, and Eq. (4) must be generalized.

The zero-wave-vector plasmon spectrum can be calculated from optical data even though the photons do not excite these plasmons. The quantity

$$-\text{Im}(\tilde{\epsilon}^{-1}) = \epsilon_2 / (\epsilon_1^2 + \epsilon_2^2) \quad (5)$$

is a measure of the probability that a normally incident charged particle will excite a long-wavelength plasmon

and hence lose an energy equal to the plasmon energy.^{7,8} It will be called the energy-loss function (ELF). For a free-electron gas described by Eq. (3), the ELF peaks at ω_p . The width and height of the ELF peak are determined by the lifetime of the plasmons. (Peaks in the ELF due to one-particle excitations will not occur in our samples in our energy range.) $\text{Im}(\tilde{\epsilon}^{-1})$ can be found from the optical constants measured by conventional techniques² or by optical techniques in which $\text{Im}(\tilde{\epsilon}^{-1})$ is measured directly,⁹⁻¹¹ and agreement with measurements of energy losses of electrons passing through films is reasonably good.^{12,13}

The noble metals have similar band structures. Their optical properties should have some features in common. All have filled d bands several eV below the Fermi level. The Fermi surfaces of these metals contact the Brillouin-zone face in the $\langle 111 \rangle$ directions, around the point L . $\epsilon_2(\omega)$ for copper has two prominent low-energy peaks, at 2.2 and 4.8 eV, while that for silver has but one, at 4.3 eV. In a paper that stimulated considerable work on the optical properties of the noble metals, Ehrenreich and Philipp² interpreted their measurements of the optical constants of Cu and Ag, using the band structures calculated by Segall.¹⁴ In Cu, the first peak in ϵ_2 was ascribed to transitions from the d band to the Fermi surface near $L(L_3-L_2)$ and the second peak was associated with transitions from the d band to the conduction band (X_5-X_4) and to transitions from the Fermi surface, or just below it, at or near L to empty conduction bands. The calculated level of the highest filled d band in silver was unreliable, so they assumed a similar order of transitions in silver, adjusting the position of the d band so that the L_3-L_2 transition came at the observed edge energy. The L_2-L_1 transition then occurred some 2 eV above the edge.

This interpretation was questioned by several people. Berglund and Spicer¹⁵ interpreted their photoemission data by assuming that transitions from the d band did not conserve wave vector. (Optical transitions will be described as "direct," in which the wave vector of the excited electron is conserved, "indirect," in which the wave vector of the excited electron changes due to momentum exchange with phonons or impurities, and "nondirect," in which the wave vector of the initial or final electronic state is not a well-defined quantity.^{15,16}) Berglund and Spicer also assigned a large role to

⁸ H. Frohlich and H. Pelzer, Proc. Phys. Soc. (London) **A68**, 525 (1955).

⁹ S. Yamaguchi, J. Phys. Soc. Japan **17**, 1172 (1962).

¹⁰ S. Yamaguchi, J. Phys. Soc. Japan **18**, 266 (1963).

¹¹ A. J. McAlister and E. A. Stern, Phys. Rev. **132**, 1599 (1963).

¹² H. Raether, *Springer Tracts in Modern Physics* (Springer-Verlag, Berlin, 1965), Vol. 38, p. 84, and references therein.

¹³ M. Creuzberg, Z. Physik **196**, 433 (1966).

¹⁴ B. Segall, Phys. Rev. **125**, 109 (1962); General Electric Research Laboratories Report No. 61-R1 (2785G), 1961 (unpublished).

¹⁵ C. N. Berglund and W. E. Spicer, Phys. Rev. **136**, A1044 (1964).

¹⁶ W. E. Spicer, Phys. Rev. **154**, 385 (1967).

⁵ H. E. Bennett and J. M. Bennett, in *Optical Properties and Electronic Structure of Metals and Alloys*, edited by F. Abeles (North-Holland Publishing Co., Amsterdam, 1966), p. 175.

⁶ C. B. Wilson, Proc. Phys. Soc. (London) **76**, 481 (1960).

⁷ F. Stern, Solid State Phys. **15**, 299 (1963).

transitions near $L_{2'}-L_1$ in the 4.8- and 4.3-eV peaks in Cu and Ag, respectively. To reinforce the original interpretation of Ehrenreich and Philipp,² Cooper, Ehrenreich, and Philipp,¹⁷ and Haga and Okamoto¹⁸ calculated $\epsilon_2^b(\omega)$ for direct transitions near $L_3-L_{2'}$ and achieved what was considered good agreement with experiment. However, Beaglehole^{3,19} pointed out that the constant oscillator strength assumed in the previous calculations could be in error. He showed that several other transitions could easily contribute appreciably to ϵ_2^b in the region of the peaks and that the correct assignment of transitions to the observed structure in ϵ_2 is not straightforward even if one has a reliable energy-band diagram. Specifically, he suggested the $L_{2'}-L_1$ transitions should contribute appreciably to the peak previously ascribed to X_5-X_4 .

Recently, Mueller and Phillips⁴ made a detailed calculation of $\epsilon_2^b(\omega)$ for Cu, including energy-dependent matrix elements. As noted by Beaglehole, at any one energy, transitions from several parts of the Brillouin zone were found to contribute to ϵ_2^b . The edge in ϵ_2^b at 2.1 eV arises from transitions near $L_3-L_{2'}$, while the peak at 4.8 eV arises partly from $L_{2'}-L_1$ transitions as suggested by Beaglehole, and partly from L_1 (d band)- $L_{2'}$ (Fermi surface) transitions, not from transitions at X . The 2.2-eV peak was ascribed to a virtual exciton resonance, a many-body effect which may be Spicer's nondirect transitions. These transition assignments have been made more certain by recent piezoreflectance measurements.²⁰ Mueller and Phillips suggest that the peak at 4.3 eV in ϵ_2 for silver arises from a strong $L_3-L_{2'}$ transition and a weak $L_{2'}-L_1$ transition which overlap. The $L_{2'}-L_1$ transitions lie at about the same energy in both metals because the conduction bands are similar. The $L_{2'}-L_1$ transitions are weaker in silver than in copper because the neck of the Fermi surface is smaller in the former. The $L_3-L_{2'}$ transition shifts to higher energy in silver because of the deeper-lying d band. Thus the first interband edge in silver is expected to arise from two types of transition near L .

BAND STRUCTURE AND OPTICAL PROPERTIES OF NOBLE-METAL ALLOYS

Several models for the band structures of dilute disordered alloys have been suggested. The rigid-band model^{21,22} assumes that the perturbation caused by the

solute simply shifts all the energy eigenvalues of the solvent by a constant amount. The band structure thus shifts rigidly in energy. If the solute valence differs from that of the solvent, the Fermi level shifts with respect to the bottom of the conduction band by an amount determined by the density of states of the solvent. The model of Freidel²³ emphasizes the distribution of electrons in real space rather than in wave-vector space. It considers the screening by conduction electrons of the excess charge on the solute atoms, leading to very small changes in the Fermi level. Finally, Cohen and Heine²⁴ have proposed a model in which the electron energy gaps at the $\langle 111 \rangle$ zone faces change with alloying in a manner which can be estimated from atomic parameters. The gap changes result in an altered Fermi surface and density of states.

Recent measurements of the optical properties of α -phase Cu-Zn have been made by Biondi and Rayne²⁵ and by Bailey and Langstroth.²⁶ The first interband absorption edge and peak in ϵ_2 of pure copper shifts to higher energy as zinc is added. If the transition assigned by Ehrenreich and Philipp to this peak is correct, the rigid-band model qualitatively, but not quantitatively, describes the shift. As Biondi and Rayne point out, Freidel's theory does no better. The second peak in ϵ_2 shifts to lower energy with increasing Zn content. The rigid-band model again is qualitatively correct if this peak arises from transitions from the Fermi surface to a higher conduction band, as originally suggested by Mott and Jones,²² but the X_5-X_4 transitions proposed by Ehrenreich and Philipp require the d band to move upward with respect to the free-electron conduction band. Lettington²⁷ has shown how the rigid-band model can fit the data, by keeping the d band fixed but letting the conduction band drop upon alloying. However, it now seems likely⁴ that the X_5-X_4 transition Lettington used is not responsible for this peak. The virtual exciton resonance atop the $L_3-L_{2'}$ one-electron transition⁴ washes out as Zn is added to Cu.^{27,28}

Green²⁹ has measured the reflectivity of bulk samples of Ag and of α -phase alloys of Ag with Zn and Cd. A dispersion analysis gave $\tilde{\epsilon}$. We shall discuss some of his Ag-Cd results along with our Ag-In results.

Amar and Johnson^{30,31} have carried out a band-

¹⁷ B. R. Cooper, H. Ehrenreich, and H. Philipp, Phys. Rev. **138**, A494 (1965).

¹⁸ E. Haga and H. Okamoto, J. Phys. Soc. Japan **20**, 1610 (1965).

¹⁹ D. Beaglehole, in *Optical Properties and Electronic Structure of Metals and Alloys*, edited by F. Abeles (North-Holland Publishing Co., Amsterdam, 1966), p. 154.

²⁰ U. Gerhardt, D. Beaglehole, and R. Sandrock, Phys. Rev. Letters **19**, 309 (1967).

²¹ H. Jones, Proc. Roy. Soc. (London) **A144**, 225 (1934); **A147**, 396 (1934).

²² H. F. Mott and H. Jones, *The Theory of the Properties of Metals and Alloys* (Dover Publications, Inc., New York, 1958), p. 170.

²³ J. Freidel, Advan. Phys. **3**, 464 (1954).

²⁴ M. H. Cohen and V. Heine, Advan. Phys. **7**, 395 (1958).

²⁵ M. A. Biondi and J. A. Rayne, Phys. Rev. **115**, 1522 (1959).

²⁶ R. C. Bailey and G. F. O. Langstroth, Bull. Am. Phys. Soc. **12**, 704 (1967); and private communication.

²⁷ A. H. Lettington, Phil. Mag. **11**, 863 (1965).

²⁸ J. A. Rayne, in *The Fermi Surface*, edited by W. A. Harrison and M. B. Hebb (John Wiley & Sons, Inc., New York, 1960), p. 266.

²⁹ E. L. Green, Ph.D. thesis, Temple University, 1965 (unpublished) (copy obtainable from University Microfilms, Inc., Ann Arbor, Mich., No. 66-652).

³⁰ H. Amar and K. Johnson, in *Optical Properties and Electronic Structure of Metals and Alloys*, edited by F. Abeles (North-Holland Publishing Co., Amsterdam, 1966), p. 586.

³¹ H. Amar, K. H. Johnson, and C. B. Sommers, Phys. Rev. **153**, 655 (1967).

structure calculation for α Cu-Zn, assuming the d band is not sensitive to Zn concentration. Their bands show that the d -band-to-Fermi-surface transition should shift to higher energy and the L_2 - L_1 transition to lower energy, as predicted by the Cohen and Heine theory, both shifts being in good agreement with the data of Biondi and Rayne.

The effects of alloying on the nature of the collective oscillations has not often been studied. Besides Green's work, Sueoka and co-workers^{32,33} have studied Ag-Au alloys, while Muldawer and Goldman³⁴ have studied β -phase Cu-Zn alloys.

EXPERIMENTAL METHOD

Samples

Bulk samples of Ag-In alloys were produced by arc melting. Several samples of each were chemically analyzed, and measurements of the lattice parameter were made. Small pieces of alloy were placed in resistance-heated tantalum boats in an ion-pumped, viton-sealed vacuum evaporator. By outgassing the boat and alloy before evaporation, evaporation was carried out at a pressure of 2×10^{-8} Torr. Films about 1000–1600 Å thick were evaporated in about 30 sec on fused quartz substrates at room temperature. The substrates were protected by a shutter during outgassing. Simultaneously, a curved glass substrate closer to the boat received a film about 3000 Å thick, to be used for lattice-parameter determinations. All films were annealed in the vacuum chamber for 3 h at 300°C. This was necessary to produce sharp x-ray diffraction lines.

The composition of a film was determined by comparing the lattice parameter of the film with that of bulk samples of known composition. The films tended to be deficient in indium compared to the bulk samples. Differences in the vapor pressures of silver and indium caused the preferential loss of indium during outgassing. Table I lists the starting material and film compositions. The uncertainties in composition represent the spread in the results of repeated composition measurements. At higher indium compositions, the broader diffraction lines increased the error in composition. Reannealing did not sharpen the diffraction lines.

After the optical measurements had been made, the film thicknesses were measured on a Varian multiple-beam interferometer with an accuracy of ± 30 Å.

Optical Measurements

Measurements of the reflectance R and transmittance T were made on a Cary 14R spectrophotometer using a

³² O. Sueoka and E. Fujimoto, J. Phys. Soc. Japan **20**, 569 (1965).

³³ H. Fukutani and O. Sueoka, in *Optical Properties and Electronic Structure of Metals and Alloys*, edited by F. Abeles (North-Holland Publishing Co., Amsterdam, 1966), p. 565.

³⁴ L. Muldawer and H. G. Goldman, in *Optical Properties and Electronic Structure of Metals and Alloys*, edited by F. Abeles (North-Holland Publishing Co., Amsterdam, 1966), p. 574.

TABLE I. Alloy concentrations (at. % In).

| Starting material | Film |
|-------------------|----------|
| 1.21 | 0.5±0.1 |
| 2.26 | 1.0±0.1 |
| 3.16 | 1.7±0.12 |
| 4.82 | 2.4±0.15 |
| 6.38 | 4.1±0.3 |

spectral band pass of 0.023 eV. The reflectance measurements were made using a reflectance attachment similar to that described by Hartman and Logothetis.³⁵ Silver films as thick as 2000 Å transmit a measurable amount around the reflectance minimum at 3.8 eV. We measured the reflectance and transmittance with the beam incident from the substrate. This is necessary because the most important term in the expression for the reflectance of the film, $R = f(n, k, n_0)$, where $\tilde{N} = n - ik$ is the complex refractive index of the film and n_0 is the refractive index of the dielectric from which the light strikes the film, is independent of n when $n^2 = n_0^2 + k^2$. For silver, if $n_0 = 1$ (air), this occurs for $\lambda \approx 3200$ Å, and the errors in n and k , as a result of small errors in R and T , become intolerable for $\lambda \lesssim 3200$ Å. If $n_0 \approx 1.5$ (quartz), the errors are large only for $\lambda \lesssim 3050$ Å. (This phenomenon has been discussed by Grant and Paul.^{36,37}) In finding n and k from the transmittance and reflectance, multiple reflections in the film and substrate were considered, as was reflection at the air-substrate interface. n and k can be obtained from expressions for the reflectance and transmittance of the sample derived from multiple application of the Fresnel equations. However, since these equations cannot be solved analytically, a numerical, iterative technique was used on an IBM 360 computer.

Similar measurements were also made at liquid-helium temperature. The samples were placed in an exchange gas and were at 4.4 or 4.5°K. The accuracy of the measurements is discussed in the Appendix.

RESULTS

The curves of n and k for a film of pure silver are shown in Fig. 1 along with those of Huebner *et al.*³⁸ The agreement is good. Their film was deposited on a quartz substrate in a vacuum of about 10^{-6} Torr and not removed until after their measurements. They obtained n and k from measurements of the reflectance at two angles of incidence. Our film was exposed to air, but the measured reflectance was determined more by the substrate-film interface than by the air-film interface. Thus, although our films probably did not have clean surfaces, we believe that this does not have much effect

³⁵ P. L. Hartman and E. Logothetis, Appl. Opt. **3**, 255 (1964).

³⁶ P. M. Grant and W. Paul, J. Appl. Phys. **37**, 3110 (1966).

³⁷ P. M. Grant, Harvard University Division of Engineering and Applied Physics Gordon McKay Laboratory Technical Report No. HP-14, 1965 (unpublished).

³⁸ R. H. Huebner, E. T. Arakawa, R. N. Hamm, and R. A. MacRea, J. Opt. Soc. Am. **54**, 1434 (1964).

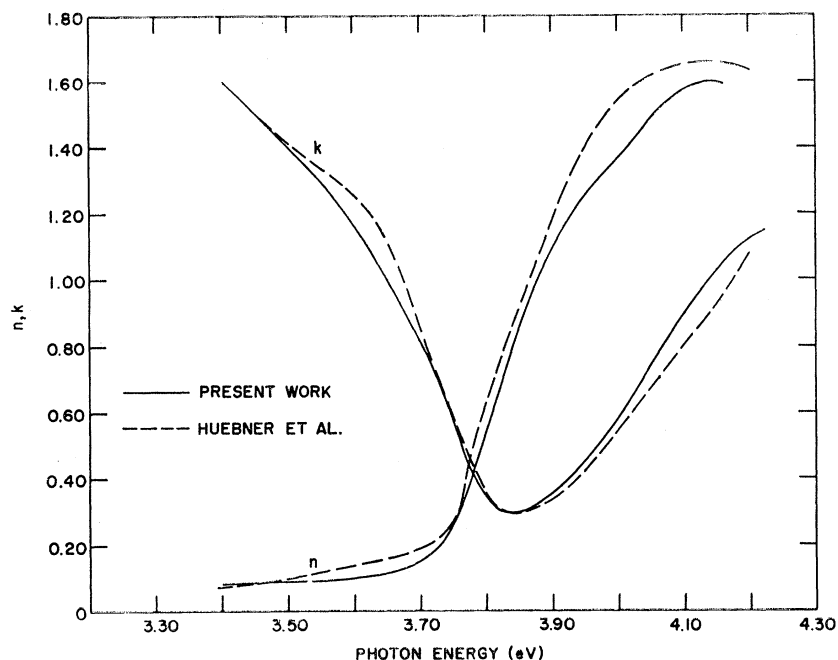


FIG. 1. Real and imaginary parts of the refractive index of silver films at 300°K. Solid lines: present work (data for one film); dashed lines: Ref. 38.

on our data. As shown in Ref. 38, the optical properties of good, thick films of silver differ from those of bulk silver, especially around 3.8 eV. The differences are primarily in the magnitude of the optical constants, and not their spectral dependences. The principal difference between the optical constants of films and of bulk silver is that the minimum value of k is about twice as large in the films. The consequences of this are particularly striking in the height of the peak of $-\text{Im}(\bar{\epsilon}^{-1})$. Thus we believe the results of alloying on the optical properties of

silver can be studied in films, at least in films as thick as ours, as long as the absolute magnitudes of the optical constants are not used in the interpretation.

Figures 2 and 3 show n and k for silver and the five Ag-In alloys. There is a regular variation of the curves with composition, except above 4.1 eV for the n curve for 1.7% In. Each curve represents the average of the results for three simultaneously evaporated films of different thickness. Figures 4-6 exhibit the real and imaginary parts of the dielectric constant ($\epsilon_1 = n^2 - k^2$,

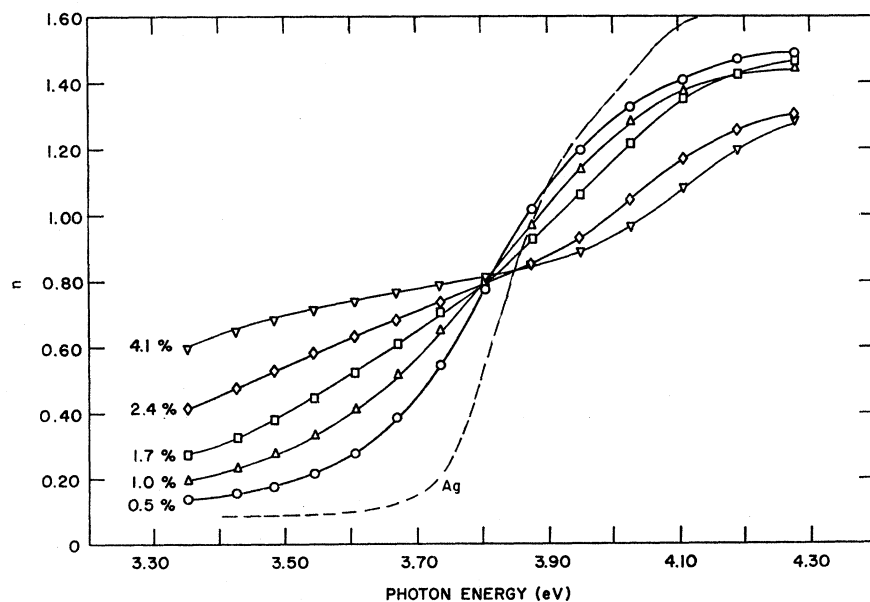


FIG. 2. Real part of the refractive index for silver and five Ag-In alloys at 300°K.

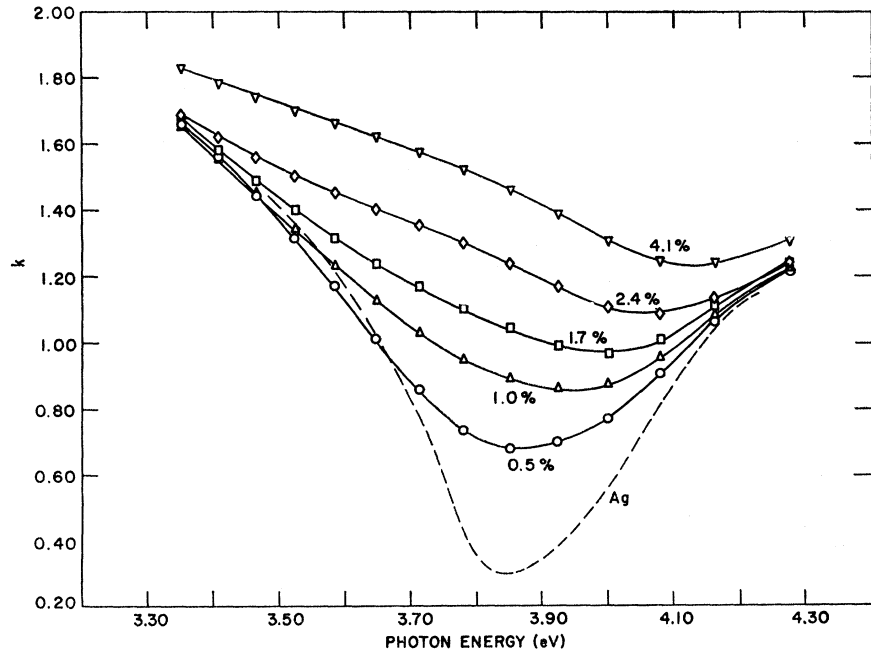


FIG. 3. Imaginary part of the refractive index for silver and five Ag-In alloys at 300°K.

$$\epsilon_2 = 2nk$$

$$= 2nk / (n^2 + k^2)^2.$$

and the energy-loss function $-\text{Im}(\tilde{\epsilon}^{-1})$. The data taken at 4.4°K do not differ much from the

room-temperature data for the alloys, although there is some change for silver. Because of the great similarity of data at both temperatures, we display only ϵ_2 and

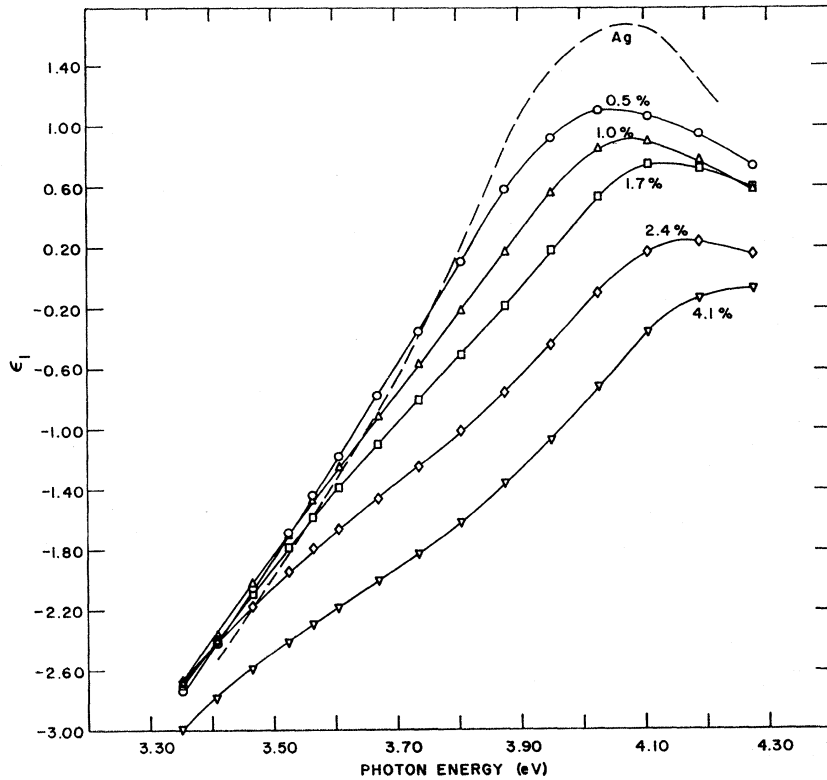


FIG. 4. Real part of the dielectric constant ϵ_1 for silver and five Ag-In alloys at 300°K.

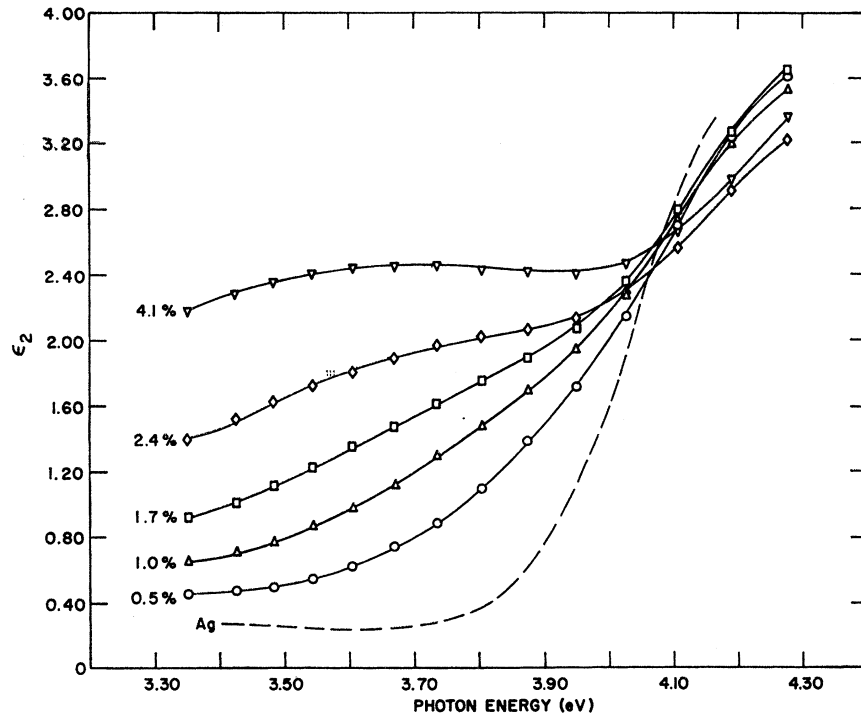


FIG. 5. Imaginary part of the dielectric constant ϵ_2 for silver and five Ag-In alloys at 300°K.

$\text{Im}(\tilde{\epsilon}^{-1})$ (Figs. 7 and 8). These data were obtained on only one film of each alloy, and are less accurate than the room-temperature data.

DISCUSSION

It is useful to separate $\tilde{\epsilon}$ into free-carrier and interband parts. Expanding ϵ_2^f to first order in $(\omega\tau)^{-1}$, we get

$$\epsilon_2^f(\omega) = (\omega_p^2/\omega^2)(1/\omega\tau). \quad (6)$$

Just below the first interband edge we expect ϵ_2^f to be small, decreasing with increasing photon energy, while interband effects, when they begin, contribute to ϵ_2 a term that increases with increasing photon energy. Figure 5 shows that at our lowest photon energy, 3.35 eV, ϵ_2 for silver decreases with increasing photon energy, while for the 0.5% In alloy, and perhaps the 1.0%-In alloy, ϵ_2 has a minimum. Hence there is interband absorption at our lowest photon energy in all the alloys. As a rough estimate of the free-carrier contribution to ϵ_2 , we use Eq. (6). τ^{-1} can be approximated by a sum of terms due to various scattering processes, at least for low frequencies, and one of them, due to impurity scattering, is proportional to c , the impurity concentration. We assume this holds at optical frequencies as well and assume that the impurity scattering rate is linear in c , even for $c \sim 5\%$. Solving Eq. (6) for τ of our pure-silver films, using ϵ_2 at 3.35 eV, we get $\tau = 5.7 \times 10^{-15}$ sec, considerably less than the value found at about this frequency for bulk silver,² 16×10^{-15} sec. This is a consequence of the larger values of \hbar in the films,³⁸

and may be a result of the strain in the films, even after annealing.³⁹ For the alloys, we assume that the part of τ^{-1} proportional to c can be obtained from the dc resistivity measurements on Ag-In alloys by Linde.⁴⁰ This term is added to the τ^{-1} for our silver films to give a τ for each alloy. Equation (6) is then evaluated at all energies of interest to give ϵ_2^f , which is subtracted from the measured ϵ_2 . The quantity ϵ_1^f can be obtained from Eq. (2) or Eq. (3) and is insensitive to the above assumptions about τ . The resultant ϵ_1^b and ϵ_2^b are shown in Figs. 9 and 10. The ϵ_2^b curves will be a bit too high at high photon energies if τ becomes shorter at these energies.

The curve of ϵ_1^b for pure silver rises monotonically from a constant value at low energies to a peak at 4.03 eV. As indium is added, the peak in ϵ_1^b shifts to higher energy, while ϵ_1^b grows at energies below 4.03 eV, and eventually the ϵ_1^b -versus-energy slope becomes negative between 3.3 and 3.7 eV for the 4.1% alloy. This is indicative of a broad, weak peak in ϵ_1^b at an energy below 3.3 eV. Such behavior also occurs in Ag-Cd at about 10% Cd.²⁹ The steep edge in ϵ_2^b at about 3.9 eV splits into two components as indium is added. The stronger component shifts to higher energy and the weaker component shifts to lower energy. At 2.4 and 4.1% In, the low-energy component appears as a shoulder on the absorption edge. The peak of this shoulder, if we subtract off an extrapolated edge, is in

³⁹T. B. Light and C. N. J. Wagner, J. Vac. Sci. Tech. 3, 1 (1966).

⁴⁰J. O. Linde, Ann. Physik 14, 353 (1932).

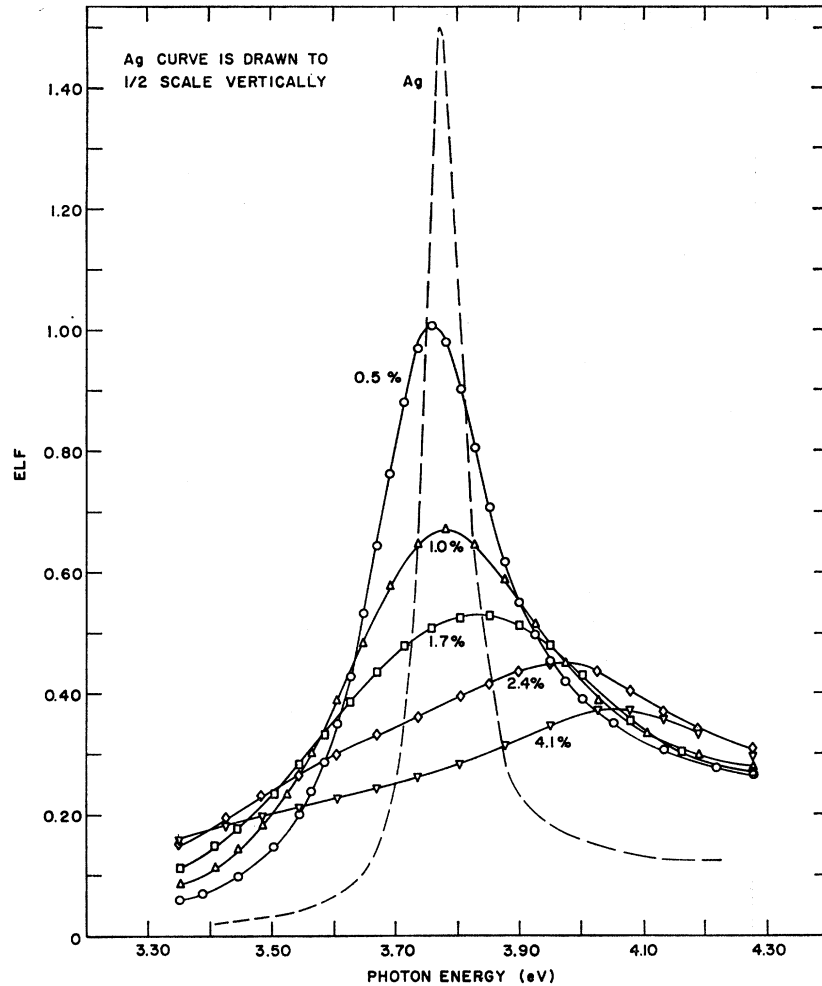


FIG. 6. Energy-loss function $-\text{Im}(\bar{\epsilon}^{-1})$ for silver and five Ag-In alloys at 300°K. Note scale change for the silver curve.

the vicinity of 3.7 eV, and the low-energy tail extends to below 3.3 eV. In several other measurements, a weak peak in ϵ_2 at 3.5 eV has been reported.^{29,41} This peak is even more pronounced in piezoreflectance measurements.⁴² There is a hint of such a peak in our data for pure silver, and in those of Ref. 38 as well, but it seems unrelated to the structure that separates from the edge as indium is added.

Considering now only the ϵ_2^b curves, we associate the strong edge, which shifts to higher energy upon alloying, with d -band-to-Fermi-surface transitions (near $L_3-L_{2'}$) and the weak transition, which shifts to low energy upon alloying, to $L_{2'}-L_1$ transitions or to transitions from the Fermi surface near $L_{2'}$ to higher conduction-band states near L_1 . (We do not believe these represent indirect transitions with indium ions conserving momentum, for reasons stated later.) Both transitions shift with indium concentration in the same fashion as the corresponding transitions in copper shift with zinc concentration.^{4,25,26}

⁴¹ G. Joos and A. Klopfer, Z. Physik **138**, 251 (1954).

⁴² M. Garfinkel, J. J. Tiemann, and W. E. Engeler, Phys. Rev. **148**, 695 (1966).

We cannot make a quantitative comparison in the two metals because of overlapping structure in ϵ_2^b . Green²⁹ has observed the shift of the $L_3-L_{2'}$ peak in silver as Cd and Zn are added. The rigid-band model, with the $L_3-L_{2'}$ gap kept constant, accounts for the shift up to about 30%-Cd concentration and up to 10%-Zn concentration. The $L_3-L_{2'}$ gap must diminish considerably at higher concentrations to give agreement²⁹ with the rigid-band model.

From the shape of the peaks in ϵ_1^b with alloying, it is clear that not only does the $L_3-L_{2'}$ transition shift to higher energy with alloying, but it broadens due to an increase in interband damping, to the uncertainty in wave vector of states in the alloy, to changes in the many-body process which may contribute to the peak, or a combination of these. If we can assume a rigid-band model, we can estimate the shift in the onset of this transition with alloying by using the electronic specific heat of pure silver. (The effects of alloying on the electronic specific heat are small,⁴³ and considering them

⁴³ B. A. Green and H. V. Cuthbert, Phys. Rev. **137**, A1168 (1965).

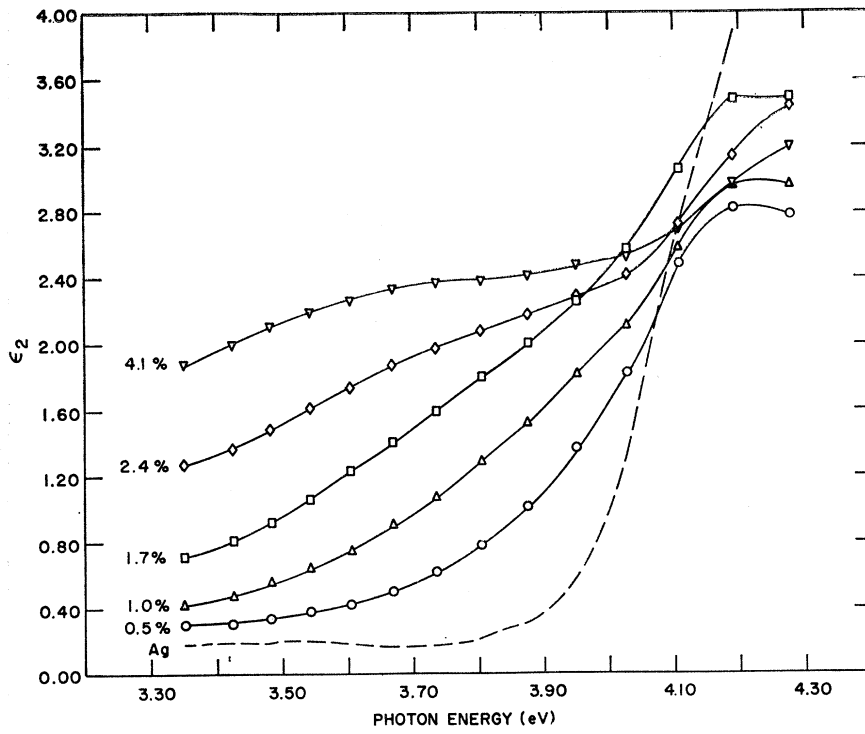


FIG. 7. Imaginary part of the dielectric constant ϵ_2 for silver and five Ag-In alloys at 4.4°K.

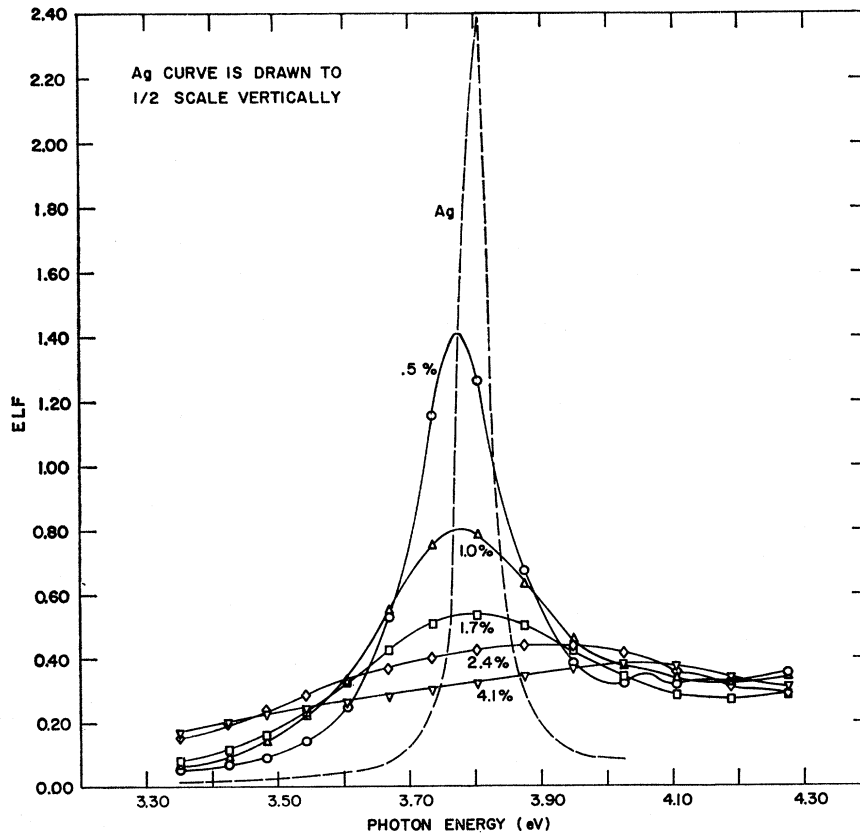


FIG. 8. Energy-loss function $-\text{Im}(\epsilon^{-1})$ for silver and five Ag-In alloys at 4.4°K. Note scale change for the silver curve.

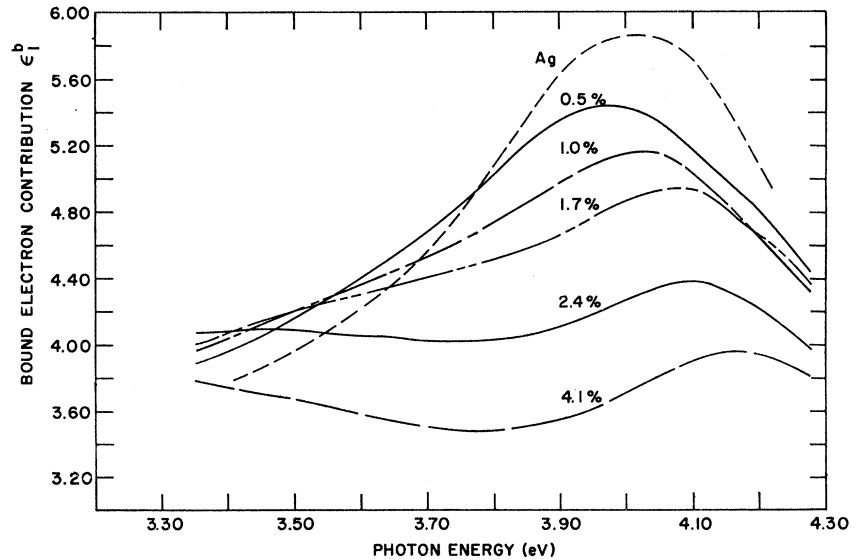


FIG. 9. Interband contribution to the real part of the dielectric constant ϵ_1^b for silver and five Ag-In alloys at 300°K.

gives a very small correction to our estimate.) From Green and Cuthbert's value⁴³ of the specific heat, one finds that the Fermi level should shift linearly above the energy at $L_{2'}$ with increasing indium concentration, for small enough concentrations, and this shift is +0.29 eV for 4.1% In. This is the shift predicted by the simplest version of the rigid-band model. In fact, the energy of the point $L_{2'}$ could shift with respect to the d band.²⁷ By extrapolating the absorption edges in Fig. 10, one finds

a negative shift, but as Fig. 9 clearly shows, this result is affected by increased broadening of the edge in the alloys. The extrapolated high-energy peak in ϵ_2^b and the peak in ϵ_1^b show positive shifts with alloying. Ideally one would like to see the onset of the interband edge for comparison with band structures. Even if the underlying, weaker transition could be ignored, the broadening of the edge upon alloying precludes this. Unfortunately, the shift of the peak in ϵ_2^b with alloying may result from

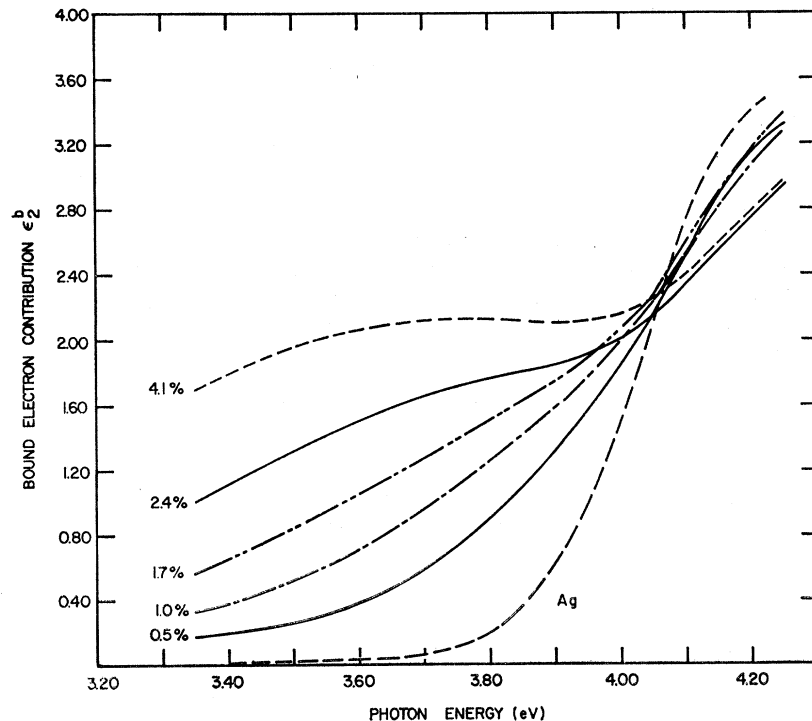


FIG. 10. Interband contribution to the imaginary part of the dielectric constant ϵ_2^b for silver and five Ag-In alloys at 300°K, assuming ϵ_2^f can be calculated from dc resistivity data on alloys (see text).

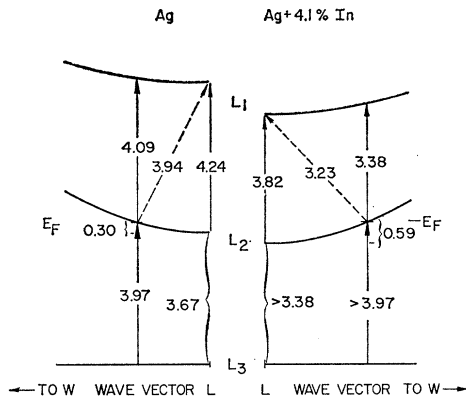


FIG. 11. Schematic energy bands near L for silver (left) and $\text{Ag}+4.1\% \text{In}$ (right). The numbers are energies in eV. The d band is assumed flat and energies are measured with respect to it (at L_3). The bands and Fermi level E_F for silver are consistent with calculations, optical data, and the measured Fermi surface. The curvature of the upper conduction band is not known, but band-structure calculations indicate that it is less than that of the lower conduction band. The shift of the $L_{2'}-L_1$ gap upon alloying is from the theory of Cohen and Heine. The shift of the Fermi level was calculated from the electronic specific heat. The shift of $L_{2'}$ with respect to L_3 is not known, but the d band to Fermi-surface transition occurs at $\hbar\omega > 3.97$ eV. The dashed transitions are the lowest-energy indirect transitions. The solid transitions are direct.

changes in matrix elements, in the joint density of states, as well as in the energy bands and Fermi energy.

Turning now to the $L_{2'}-L_1$ transitions, we first assert that the low-energy edge arises from direct (rather than indirect) transitions from the Fermi surface near $L_{2'}$, instead of from $L_{2'}$ itself. A combination of band-structure calculations and experimental data¹⁷ gives the energies listed in the left half of Fig. 11 for silver. Although the accuracy of the energies labeled in the figure is unknown, the relative energies should be fairly good, and because of the relative curvatures of the two conduction bands, the direct transition from the Fermi surface occurs at lower energy than the direct transition from $L_{2'}$. This conclusion is valid for the bands resulting from the use of either the Hartree or Hartree-Fock potential used by Segall and is probably true for the real band structure of silver. The edge of the direct absorption from near $L_{2'}$ thus begins with the transition from the Fermi surface. Indirect transitions from the Fermi surface to L_1 could occur upon alloying,⁴⁴ with wave vector being conserved by the impurity ion. For very small impurity concentrations such transitions would begin at 3.94 eV, as shown by the dotted line in the left half of Fig. 11, and continue to the edge at 4.09 eV. We believe such transitions do not occur for several reasons. First, the absorption that splits from the main edge into the region below 3.9 eV has a peak in it. Indirect transitions should not show a peak in such a limited energy range for the bands involved. Second, the data of Green²⁹ show this peak continuing to grow with concentration of Cd or Zn. At 30% solute concentration

the split-off peak in ϵ_2 exceeds the original ϵ_2 peak in pure silver. Its splitting is of the same sign and magnitude as the corresponding, but stronger, transition in Cu-Zn.

[*Note added in proof.* Piezoreflectance measurements have just been completed on Ag-In films [C. E. Morris and D. W. Lynch (to be published)] which indicate that the direct $L_{2'}-L_1$ gap is 4.06 eV in pure silver and drops to 3.35 eV for $\text{Ag}+5\% \text{In}$. There is evidence of a long tail of indirect transitions, beginning at 2.8 eV in a 4.1%-In alloy. Most of ϵ_2^b in Fig. 10 arises from direct transitions. The indirect transitions occur at still lower energies.]

The onset of a rise in ϵ_2^b is well below 3.3 eV (Fig. 10) in the 2.5 and 4.1% alloys. This conclusion does not rest on the assumption about τ used to obtain ϵ_2^b . The curves of ϵ_2 (Fig. 5) also suggest this. The expected rise in the Fermi level for a 4.1% alloy is 0.29 eV, and on the basis of a rigid-band model, the direct transition near $L_{2'}-L_1$ should shift less than this because both conduction bands have similar curvatures. The shift observed is clearly larger than 0.6 eV, implying that the $L_{2'}-L_1$ gap decreases somewhat upon alloying. The theory of Cohen and Heine²⁴ predicts a gap in the 4.1%-In alloy that is 0.42 eV smaller than that in silver, although the magnitude of the gap is not predicted correctly. Thus a shift of 0.4 to 0.8 eV in the transition is expected, while a shift of at least 0.6 eV is observed. Phillips has commented⁴⁵ that the L_1 level is generally more sensitive to changes in potential than the $L_{2'}$ and L_3 levels. Moreover, Amar *et al.*³¹ find the $L_{2'}-L_1$ gap in their calculated band structure for α brass is smaller than the gap in copper. The right-hand side of Fig. 11 shows energy bands for a 4.1%-In alloy, using the Fermi-level shift and $\langle 111 \rangle$ gap shift discussed above. It is consistent with the optical data. The indirect transition, shown dotted, would begin at 3.1 eV in this scheme.

The energy-loss function $-\text{Im}(\tilde{\epsilon}^{-1})$ describes the plasma resonance of the conduction electrons. In pure silver, the frequency is given by Eq. (4), since $\epsilon_2^b(\omega_0) \approx 0$. The peak height of the ELF is $1/\epsilon_2(\omega_0)$ and the full width at half-maximum is $2\epsilon_2(\omega_0)/[d\epsilon_1/d\omega]_{\omega_0}$ if $\epsilon_2(\omega_0) \ll 1$. Thus the height is determined only by ϵ_2 , but both ϵ_2 and $d\epsilon_1/d\omega$ determine the width. We see from Fig. 6 that alloying produces a marked drop in the peak of the ELF and large increases in the half-width. $\epsilon_2(\omega_0)$ is increased by three processes: the increase in τ of the free carriers, the broadening of the strong $L_3-L_{2'}$ transition, and the shift of the $L_{2'}-L_1$ transition toward ω_0 . At about 2.5% In, the plasma oscillations are sufficiently damped that they are not well-defined excitations of the system.

For pure silver, the zero of ϵ_1 occurs at nearly the same frequency as the peak in the ELF. The latter is the screened plasma frequency ω_0 . As we alloy, the zero of

⁴⁴ J. Ziman, *Phil. Mag.* 5, 757 (1960).

⁴⁵ J. C. Phillips, comment in *Optical Properties and Electronic Structure of Metals and Alloys*, edited by F. Abeles (North-Holland Publishing Co., Amsterdam, 1966), p. 173.

ϵ_1 moves to higher frequencies much more rapidly than the peak of the ELF. In fact, ϵ_1 for the 4.1% alloy has no zero in our energy range. This is a manifestation of the damping in the alloys. If we expand ϵ_1 and ϵ_2 about ω_0 , the frequency where ϵ_1 vanishes, i.e.,

$$\epsilon_1 = (d\epsilon_1/d\omega)_{\omega_0}(\omega - \omega_0) = S_1(\omega - \omega_0), \quad (7)$$

$$\epsilon_2 = \epsilon_2(\omega_0) + (d\epsilon_2/d\omega)_{\omega_0}(\omega - \omega_0) = \epsilon_2(\omega_0) + S_2(\omega - \omega_0), \quad (8)$$

then the peak of the ELF occurs at the frequency where the following function has a minimum:

$$f = S_1^2(\omega - \omega_0)^2 / [\epsilon_2(\omega_0) + S_2(\omega - \omega_0)] + S_2(\omega - \omega_0) + \epsilon_2(\omega_0).$$

This is

$$\omega_0' = \omega_0 - \frac{\epsilon_2(\omega_0)}{S_2} \left[1 - \frac{S_1}{(S_1^2 + S_2^2)^{1/2}} \right]. \quad (9)$$

Equation (9) replaces Eq. (4) when $\epsilon_2(\omega_0)$ is not small. For the alloys, both S_1 and S_2 are positive, $\omega_0' < \omega_0$, and the ELF peaks at a frequency lower than that for which $\epsilon_1 = 0$. This also explains an apparent anomaly in the position of the peak of the ELF for the 0.5% alloy. Both pure silver and the 0.5% alloy have about the same value of ω_0 (Fig. 6), and the values of S_1 and S_2 are nearly identical. The shift of ω_0' to lower energies for the 0.5% alloy is due to the shortened free-electron relaxation time τ which raises $\epsilon_2(\omega_0)$, and to the shift of ϵ_2^b to lower energy.

A set of measurements was made on each sample at 4.4°K in an attempt to remove all traces of thermal broadening of the edge in the silver and 0.5%-alloy samples. The accuracy is lower, especially at both ends of the wavelength range. Cooling the samples to 4.4°K should cause a volume change of -1.2% if the silver films are unconstrained by the substrate. This is to be compared with a change of -1.0% upon applying 10-kbar hydrostatic pressure and of $+1.4\%$ as a result of adding 5.8% In to silver.⁴⁶ The fact that the film is constrained to follow the very small thermal contraction of the substrate means that the film is in tension when cooled. (There may be a similar macroscopic strain at room temperature as a result of our annealing.³⁹) That the silver film is indeed constrained to contract with the substrate is shown by the work of Zallen,⁴⁷ who showed that the pressure coefficient of the ϵ_2^b edge in silver is a function of the compressibility of the substrate. As a result, we cannot compare the edges at 4.4°K with the edges at room temperature because of the shift of the ϵ_2^b edge with strain.⁴⁷ The volume changes mentioned above show that the volume change produced by alloying is not the primary reason for the shifts of absorption edges. Similar volume changes can

TABLE II. Energies (in eV) at which ϵ_1 is zero (ω_0) and at which the maximum of the ELF occurs (ω_0').

| Alloy concentration (at.% In) | Room temperature | | Liquid-helium temperature | |
|-------------------------------|------------------|-------------|---------------------------|-------------|
| | ω_0 | ω_0' | ω_0 | ω_0' |
| 0.0 | 3.78 | 3.77 | 3.80 | 3.80 |
| 0.5 | 3.79 | 3.76 | 3.79 | 3.78 |
| 1.0 | 3.84 | 3.78 | 3.82 | 3.78 |
| 1.7 | 3.91 | 3.84 | 3.87 | 3.80 |
| 2.4 | 4.05 | 3.96 | 3.99 | 3.90 |
| 4.1 | ? | 4.05 | 4.13 | 4.03 |

be produced by temperature or pressure, with smaller effects on the edge. Zallen found $(\partial E/\partial P)_T$ for the absorption edge to be positive when he compressed the silver sample. We find a positive shift of the main part of the edge when the volume is increased by adding indium.

For pure-silver films there is only a slight (40%) increase in τ at 3.35 eV, indicative of considerable non-thermal scattering at this energy in films. The interband edge sharpens and shifts to slightly higher energy, while the zero in ϵ_1 moves 0.02 eV higher in energy. The interband contributions to ϵ_1 and ϵ_2 in all alloys sharpen upon cooling, and this sharpening apparently is not reduced by strains in the films. Green's²⁹ data on single crystals indicate a similar degree of sharpening upon cooling, as do those of Joos and Klopfer⁴¹ on evaporated films. Qualitative interpretation of the low-temperature $\tilde{\epsilon}^b$ is not possible because of uncertainties in subtracting $\tilde{\epsilon}'$ from $\tilde{\epsilon}$ and larger errors in the data.

Examination of the low-temperature ELF curves reveals that peaks are higher for silver and the two most dilute alloys, and that the silver and 0.5%-alloy peaks shift to higher energies, while the peaks for the three more concentrated alloys shift to lower energies. The 1.0%-alloy peak does not shift upon cooling. Table II gives the energies at which ϵ_1 is zero. The energy where the ELF peak occurs for silver films at 4.4°K agrees with that found by Green for single crystals at 110°K.

Changes produced by cooling in ELF curves are easily explained in terms of changes in ϵ_1 and ϵ_2 , which reflect, primarily, changes in interband absorption due directly to the cooling, or to the strain caused by cooling. For instance, the silver peak shifts to higher energy because the stronger interband contribution to ϵ_1 shifts to higher energy and causes ϵ_1 to be zero at a higher energy. A reduction in both ϵ_2' and ϵ_2^b at the plasma energy means that there is less damping of the plasma oscillations, so the maximum value of the ELF is larger. The explanation of the behavior of the 0.5% alloy is similar to that for silver. At this concentration, the $L_{2'}-L_1$ transition is at lower energy and is more pronounced, moving the zero of ϵ_1 to lower energy. The shift of the absorption edge as the 1%-In alloy is cooled causes ω_0 to become lower, but because ϵ_2 is also reduced near ω_0 , absorption does not shift the peak in the ELF

⁴⁶ W. B. Pearson, *Handbook of Lattice Spacings and Structures of Metals and Alloys* (Pergamon Press, Inc., New York, 1958).

⁴⁷ R. Zallen, in *Optical Properties and Electronic Structure of Metals and Alloys*, edited by F. Abeles (North-Holland Publishing Co., Amsterdam, 1966), p. 164.

from the zero of ϵ_1 as much as it does at room temperature. Hence there is no net change in the energy location of the ELF peak for this alloy. For the remaining alloys there is a shift to lower energy of the zero of ϵ_1 as well as an increase in ϵ_2 near the plasma energy; both of these tend to shift the ELF peak to a lower energy.

APPENDIX

We attempt to assess the accuracy of our measurements. We estimate that the reflectance R can be measured to $2\frac{1}{2}\%$ at room temperature and $3\frac{1}{2}\%$ at 4.4°K , while transmittance T errors are $3\frac{1}{2}\%$ and 4% , respectively, over the central one-half of our wavelength range. These errors are expected to be systematic and should be nearly the same at all wavelengths for any one film. Calculations were made of the changes in R and T produced by changes in n and k . From these we conclude that the largest single error in k arises from the $2\frac{1}{2}\%$ error in d , the film thickness. This error is constant for

any one film and may even be about the same for all films. The errors in d and T make k accurate to about $4\frac{1}{2}\%$. (The observed maximum deviation of a value of k at any wavelength from the average for 10 Ag films was 6% .) The calculations show that the relative error in n is approximately 10 times the relative error in R over the central half of our wavelength range. Thus n should be uncertain to about 25%, but the maximum single deviation from the average for nine Ag films was 10% for photon energies below 4.0 eV. The errors in n diminish upon alloying and for the 4.2%-In alloy, the relative errors in R and n are about equal. The actual systematic errors may not have been as large as predicted because our results agree well with those of Ref. 38, measured by quite a different technique. Above 4.0 eV the accuracy suffers greatly because of the form of the equations for n and k in terms of R and T . Of 10 Ag films, only one, that used for Fig. 1, gave data above 4.0 eV in agreement with those of Ref. 39. Hence the data on alloys can be trusted only below about 4 eV.

A Quantum Dissipation Theory of Anharmonic Crystals

A. H. OPIE

Physics Department, Monash University, Clayton, Victoria, Australia

(Received 19 March 1968)

A quantum-mechanical dissipation theory is applied to the problem of anharmonic vibrations of a crystal. Equations for the anharmonic phonon creation and annihilation operators are obtained, from which may be extracted damping-constant and frequency-shift expressions. These are compared with the results of other techniques.

I. INTRODUCTION

IT is the purpose of this paper to demonstrate the application of a formal quantum-mechanical dissipation theory for the harmonic oscillator¹ to the problem of the anharmonic crystal. Anharmonicity has received direct attention from many authors²⁻¹² employing many different techniques. However, to approach

it from a dissipation theory viewpoint utilizes the attractive concept of a phonon undergoing decay as it interacts with, and loses energy to, other phonons.

The final equation of motion, which is derived in Sec. II [Eq. (2.44)], shows that in addition to damping there also exists a driving force which restores energy to the mode. As suggested by Senitzky¹ the source of this compensating effect is quantum-mechanical fluctuations without which dissipation may not properly (quantum mechanically) be treated. Just as in classical dissipation problems, the driving forces are not considered when deducing damping properties of the system; and if the aim of this paper is to calculate only these, then concern for the fluctuations is pedantic. But in Sec. III it is shown that their inclusion leads to correct commutation relations for the phonon creation and annihilation operators. The derivations of Sec. II depend on such commutation relations and therefore consideration of fluctuations is essential for consistency.

The application Senitzky envisaged was a radiation field in a microwave cavity. Consequently, although

¹ I. R. Senitzky, *Phys. Rev.* **119**, 670 (1960).

² M. Born and K. Huang, *Dynamical Theory of Crystal Lattices* (Oxford University Press, New York, 1954).

³ A. A. Maradudin and R. F. Wallis, *Phys. Rev.* **120**, 442 (1960), paper I.

⁴ A. A. Maradudin and R. F. Wallis, *Phys. Rev.* **123**, 777 (1961), paper II.

⁵ R. F. Wallis and A. A. Maradudin, *Phys. Rev.* **125**, 1277 (1962), paper III.

⁶ A. A. Maradudin and A. E. Fein, *Phys. Rev.* **128**, 2589 (1962).

⁷ R. A. Cowley, *Advan. Phys.* **12**, 421 (1963).

⁸ B. V. Thompson, *Phys. Rev.* **131**, 1420 (1963).

⁹ K. N. Pathak, *Phys. Rev.* **139**, 1569 (1965).

¹⁰ K. S. Viswanathan and Keiji Watanabe, *Phys. Rev.* **149**, 614 (1966).

¹¹ K. Ishikawa, *Phys. Status Solidi* **21**, 137 (1967).

¹² D. C. Wallace, *Phys. Rev.* **152**, 247 (1966).